J Fluoresc (2012) 22:81–91
DOI 10.1007/s10895-011-0932-1

ORIGINAL PAPER

DFT/TDDFT Study on the Electronic Structure and Spectral Properties of Diphenyl Azafluoranthene Derivative

P. Gąsiorski · K. S. Danel · M. Matusiewicz · T. Uchacz · W. Kuźnik · A. V. Kityk

Received: 24 April 2011 / Accepted: 28 July 2011 / Published online: 19 August 2011

Abstract Paper reports the DFT/TDDFT study on the electronic structure and spectral properties of the five-membered annulated diphenyl azafluoranthene derivative 1,3-diphenyl-3*H*-indeno[1,2,3-*de*]pyrazolo-[3,4-*b*]quinoline (DPIPQ) by means of polarizable continuum model (PCM) and Onsager reaction field approaches at the B3LYP/6-31+G(d,p) level of theory. The results of calculations are compared with the optical absorption and fluorescence spectra as well as with the cyclic voltammetry data. The DFT/TDDFT/PCM approaches exhibit rather good quantitative agreement regarding the spectral position of the first absorption band; the discrepancy between the experiment and theory is less than 0.06 eV (linear response approach) or 0.25 eV (state specific approach). As for the fluorescence emission the TDDFT/PCM calculations underestimate the transition energy on about of 0.7–0.8 eV. Such discrepancy should be attributed to insufficient quality of the TDDFT/PCM optimization in the excited state. Ignoring the geometrical relaxation in the excited state provides considerably better agreement between the experiment and theory; discrepancy is less than 0.1–0.22 eV depending on a solvent polarity. The dominant influence on the fluorescence emission results mainly from the solvent reorganization in the excited state whereas the solute relaxation is indeed weak and may be ignored.

Keywords Optical absorption spectra · Fluorescence spectra · DFT and TDDFT calculations · Annulated azafluoranthene dyes

P. Gąsiorski · M. Matusiewicz · A. V. Kityk (✉)
Faculty of Electrical Engineering,
Częstochowa University of Technology,
Al. Armii Krajowej 17,
42-200, Częstochowa, Poland
e-mail: kityk@ap.univie.ac.at

K. S. Danel
Department of Chemistry, University of Agriculture,
Balicka str. 122, 30-149 Kraków, Poland

T. Uchacz
Faculty of Chemistry, Jagiellonian University,
Ingardena str. 3, 30-060 Kraków, Poland

W. Kuźnik
Chemical Department, Silesian University of Technology,
Strzody 9, Gliwice, Poland

Introduction

Progress in the heterocycle organic chemistry is indebted much to the development of novel five-membered azafluoranthenes being originally of interest of pharmacology and biotechnology, as efficient tissues oxygenators and antidepressant agents [1, 2], food technology [3], plants products [4] or compounds able to exert some biological effect such as a binding of macromolecules, particularly as efficient DNA intercalators [4, 5]. However, recent spectroscopic studies [6–10] have revealed that they may be also considered as novel efficient materials for luminescent or electroluminescence applications in blue-yellow-orange region of the visible spectra, in particular, as the dopants for polymer matrixes of electroluminescent displays or organic light emitting diodes (OLEDs) [11, 12], photovoltaic devices [13], likewise potentially promising ligands for triplet phosphors [14]. Their analogues were

also exploited in patented OLED devices [15]. The azafluoranthene dyes may be synthesized by means of the cyclization reaction from the triphenyl pyrazoloquinoline derivatives [6–9]. The latter ones represent the efficient fluorescence and electroluminescence materials, preferably in the blue region of the visible spectra. Their five-membered cyclization into the regioisomers of annulated azafluoranthenes provides a significant red shift of the optical absorption and emission spectra. Several recent works [6–9] reported the synthesis of a few new azafluoranthene derivatives likewise their optical absorption and fluorescence spectra measured in the organic solvents of different polarity. An opposite solvatochromism for the optical absorption and fluorescence is evidently a characteristic feature of these dyes. The blue (hypsochromic) shift of the first absorption band is accompanied by the red (bathochromic) shift of the fluorescence band. The opposite solvatochromism appears to be consistent with the Lippert-Mataga model based on the Onsager reaction field (ORF) approach and semiempirical evaluations (model PM3) which explains it by a specific orientation of the ground and excited state dipole moments. As for the first optical absorption band the semiempirical calculations [6–9] also give a proper magnitude of its hypsochromic shift. On the other hand, an evident problem appears with some quantitative evaluations, in particular, when the bathochromic shift of the fluorescence emission is being calculated. The analysis of the fluorescence spectra measured in solvents of different polarity suggests much larger dipole moment for the lowest excited state comparing to the one obtained within the semiempirical calculations. Corresponding discrepancy is assumed to be related either with eventual conformational relaxation of the solute in the excited state or with a mixing of neighboring excited electronic states in a specific solvent environment. Both they may modify the excited state properties including their energy and the dipole moments which are known to play a crucial role in the solvatochromic mechanism. One must be noticed, that the geometrical optimization in the excited states, even for moderately sized molecules, such as e.g. azafluoranthenes, appears to be quite problematic within the semiempirical approaches available in existing quantum-chemical software. Frequently, it results to non stable molecular structures or, alternatively, to non reasonable molecular conformations having not much to do with reality. In this respect, much more powerful calculations, including the geometry optimization, are based on the density functional theory (DFT) and its counterpart, time-dependent DFT (TDDFT) method, combined with different types of polarizable continuum models (hereafter PCMs) or solvation ORF method that most properly account an influence of the solvent shell on the solute electron structure in the ground and/or excited states.

In this paper we report a DFT/TDDFT/PCM/ORF study of the solvatochromic effect in the diphenyl derivative of annulated azafluoranthene, i.e. 1,3-diphenyl-3*H*-indeno[1,2,3-*de*]pyrazolo[3,4-*b*]quinoline (abbreviated hereafter as DPIPQ) with the chemical structure as given below:

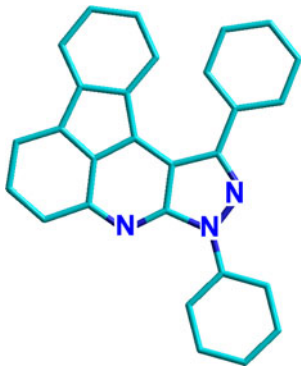

DPIPQ is characterized by nonplanar angular orientations of both aromatic rings. Recent optical spectroscopy studies of this compound [7] are completed here by cyclic voltammetry measurements directly providing the absolute energies of the HOMO and LUMO levels. The cyclic voltammetry and optical spectroscopy data are compared with the results of quantum-chemical calculations. The aim of this study is to analyze the change of the low energy electronic transitions caused by solute-solvent interaction. In spite of recent semiempirical calculations [6–8] special attention will be paid to the solute geometry relaxation in the excited state and the fluorescence emission from the equilibrium and non-equilibrium excited states. Such calculations have an evident interest from both fundamental and applied points of view. They validate different types of quantum-chemical models in order to choose the most appropriate ones for further chemical engineering, particularly related to development of novel organic dyes or fluorescent emitters with predictable spectroscopic properties.

Calculation Procedure

The DFT calculations have been performed within the quantum chemical package of programs Gaussian-09 (version B01, hereafter G09-B01) [16] using B3LYP hybrid potential with the standard 6-31+G(d,p) basis set. As for the ground state being considered its optimized molecular geometry has been obtained by DFT method. In the excited state the equilibrium geometry

was optimized by TDDFT method. The excitation and emission spectra as well as the excited state dipole moments have been calculated by means of TDDFT method. To account the solvation the DFT or TDDFT have been combined with PCM which represents so called self consistent reaction field (SCRF) approach where the cavity is created via a set of overlapping spheres covering the individual atoms of the solute. This model differs from the ORF approach used in our several recent works [6–9, 17, 18] where the solute was placed in a spherical Onsager cavity within the solvent reaction field. Within the PCM method the solvation corrections to the excitation energies may be described using basically two different methods available in Gaussian-09, known as the linear response (LR) and state specific (SS) approaches. In the standard PCM-LR method the vertical excitation with a linear response of solvation is considered. More advanced, the PCM-SS approach calculates the energy correction for a specific excited state in the reaction solvent field relevant with a chosen molecular geometry and/or state [19, 20]. Further details regarding both methods may be found in review article [21]. Both PCMs have been combined in the current study with DFT or TDDFT calculations as for the geometry optimization likewise further electronic states calculations in the gas phase or several solvents of different polarity, like a weakly polar cyclohexane (CHX), moderately polar tetrahydrofuran (THF) or strongly polar acetonitrile (ACN).

The semiempirical calculations have been performed within the quantum chemical software package Hyperchem-8.0 by means of the PM3 method, being basically used for the calculations of the excitation and emission spectra as well as the evaluations of the ground and excited state dipole moments. Despite of previous semiempirical studies [6–9] the molecular structure was optimized within the DFT/PCM or TDDFT/PCM methods and used as the input one in further semiempirical calculations. The solvation at such analysis is accounted for the simple ORF model. The electronic states were calculated using the configuration interaction (CI) method considering 24 occupied and 24 unoccupied molecular orbitals. Some other details regarding the semiempirical calculations can be found in [22–25].

Results and Discussion

Cyclic voltammetry measurements were performed by means of AUTOLAB PGSTAT20 potentiostat—galvanostat (EcoChemie, Netherlands). The platinum and silver wires (ø = 1 mm) were used as a working and quasi-reference electrodes, respectively, while the platinum coil served as an auxiliary one. The potential of quasi-reference electrode was calibrated using the ferrocene as an internal standard. 0.2 M solution of Bu_4NBF_4 (Aldrich 98% pure) in acetonitrile (POCh 99.8% HPLC grade) was used as the electrolyte. Prior to the measurements the solution was purged with argon to remove residual oxygen. The measurement consists of determining the ferrocene redox pair potential with respect to free electron in vacuum at rest [26, 27]. In the following the oxidation and reduction potentials with respect to the ferrocene redox pair were recalculated into the HOMO and LUMO energy levels. Figure 1 shows the measured voltammogram. Here the oxidation and reduction peaks, associated with the HOMO and LUMO levels, respectively, are marked by the arrows. DPIPQ exhibits the HOMO energy level at −6.194 eV and the LUMO one at −3.434 eV with the HOMO-LUMO gap ΔE_{HL} of 2.76 eV as it is summarized in the energy diagram presented in insert of Fig. 1.

Figure 2a shows the equilibrium ground state geometry of DPIPQ molecule optimized by DFT/PCM. The overall shape of the azafluoranthene moiety does not change significantly with the rising solvent polarity. Corresponding bond lengths change here less than 0.001 Å and only the angular orientation of the phenyl groups Ph1 and Ph2, characterizing by the torsion angles ϕ_1 and ϕ_2, respectively, demonstrate evident changes to more twisted orientations as the solvent polarity rises. In contrast to this, the lowest excited state, is characterized by more planar orientations of

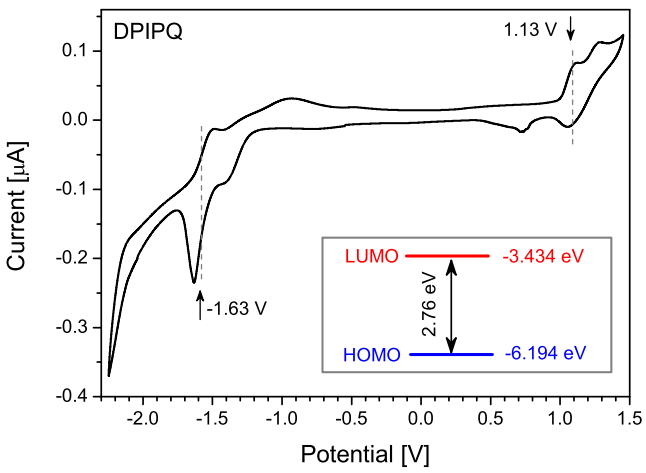

Fig. 1 Cyclic voltammogram of DPIPQ recorded in acetonitrile solution with respect to ferrocene redox couple. Reduction and oxidation peaks are marked by arrows. Insert shows the HOMO-LUMO levels as determined from the reduction and oxidation peaks

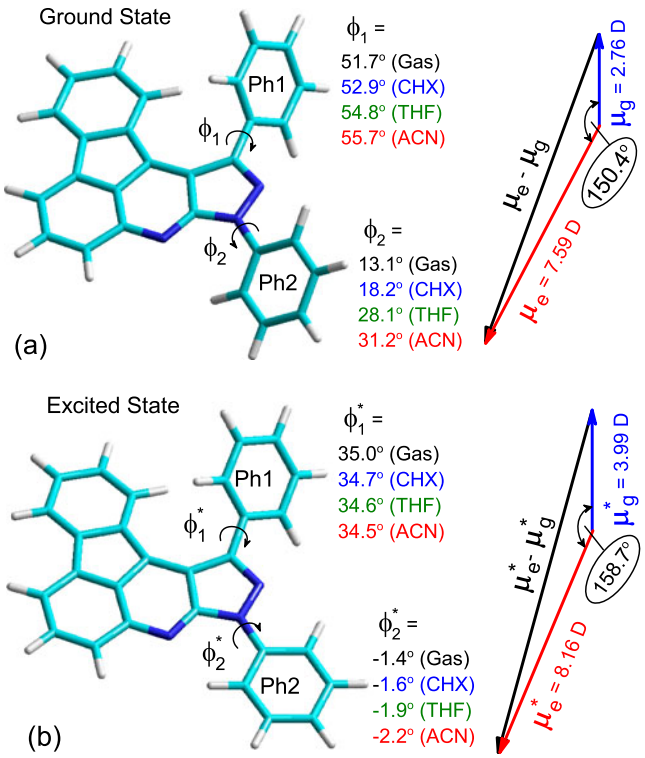

Fig. 2 The equilibrium geometries of DPIPQ molecule in the gas phase (*left*) and the vector diagrams presenting the ground (μ_g) and lowest excited (μ_e) state dipole moments (*right*). Panel **a** refers to the equilibrium ground state geometry obtained by DFT/PCM method; Panel **b** refers to the equilibrium lowest excited state geometry obtained by TDDFT/PCM method. The overall planar shape of the azafluoranthene moiety remains practically unchanged with the solvent polarity. Only the angular orientations of the phenyl groups, Ph1 and Ph2, characterizing by the torsion angles $\phi_1(\phi_1^*)$ and $\phi_2(\phi_2^*)$, respectively, demonstrate evident changes with the solvent polarity as labeled by different on-line colors

both phenyl rings, see Fig. 2b. Corresponding torsion angles, ϕ_1^* and ϕ_2^*, appear to be only weakly solvent dependent. Accordingly, upon the vertical excitation from the ground state, likewise the vertical emission from the excited state, the conformational relaxation of DPIPQ exhibits mainly the rotational dynamics of its phenyl rings by the angle of 15–30° depending on the solvent polarity. As the solvent polarity rises corresponding angular changes become more stronger. Excitation-emission cycle is accompanied also by some changes in the state dipole moments, see Fig. 2a and b, right. In particular, the relaxation in the excited state leads to their increase which thereby modifies the solvation corrections to the state energies being accounted in further DFT/TDDFT/PCM calculations.

Figure 3 presents the HOMO-LUMO energy levels determined by DFT/PCM in solvents of different polarity as well as the HOMO and LUMO orbitals [28] calculated in the gas phase of DPIPQ molecule in its equilibrium ground (panel a) or equilibrium lowest excited (panel b) states. The HOMO⇌LUMO transition exhibits only a moderate change in the charge distribution without its evident separation. Upon the excitation, a certain charge relocation takes place mainly between the phenyl rings and azafluoranthene moiety which results to a moderate magnitude of the excited state dipole moment, 7.59 or 8.16 D as for the equilibrium ground or excited state geometry, respectively. Taking together, the HOMO⇌LUMO transition should likely be interpreted as the local one rather than of the CT type. As the solvent polarity rises both HOMO and LUMO levels lower down. However, for the vertical excitation from the equilibrium solvated ground state the HOMO energy decreases faster than LUMO one resulting thereby in increase of the HOMO-LUMO gap. For the fluorescence corresponding to the vertical emission from the equilibrium solvated excited state, the HOMO-LUMO gap shrinks on

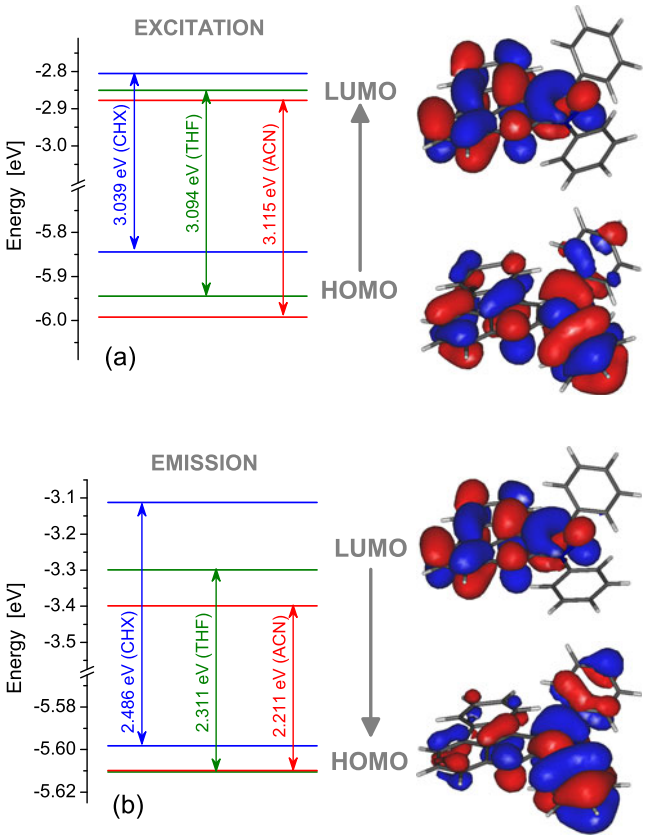

Fig. 3 HOMO and LUMO orbitals of DPIPQ as calculated by DFT method in the gas phase (*right*). HOMO and LUMO energy levels calculated by the DFT/PCM method in CHX (*blue color* online), THF (*green color* online) and ACN (*red color* online) solutions (*left*). Panels **a** and **b** correspond to excitation and emission processes, respectively

the rising solvent polarity. The opposite solvatochromic trends appear to be consistent here with the solvation blue shift of the first absorption band likewise the solvation red shift of the emission band observed in the measured spectra, see Figs. 4a, 5 and 6a. One must be emphasized that both emission or absorption processes are caused by the transitions between the singlet ground state, S_0, and the lowest excited state, S_1, consisting mainly of the HOMO⇌LUMO transition, namely by 97% at the excitation or 99% at the emission. Further interpretation refers to a specific solvation reaction field accompanying the excitation or emission processes. In particular, for the optical absorption the

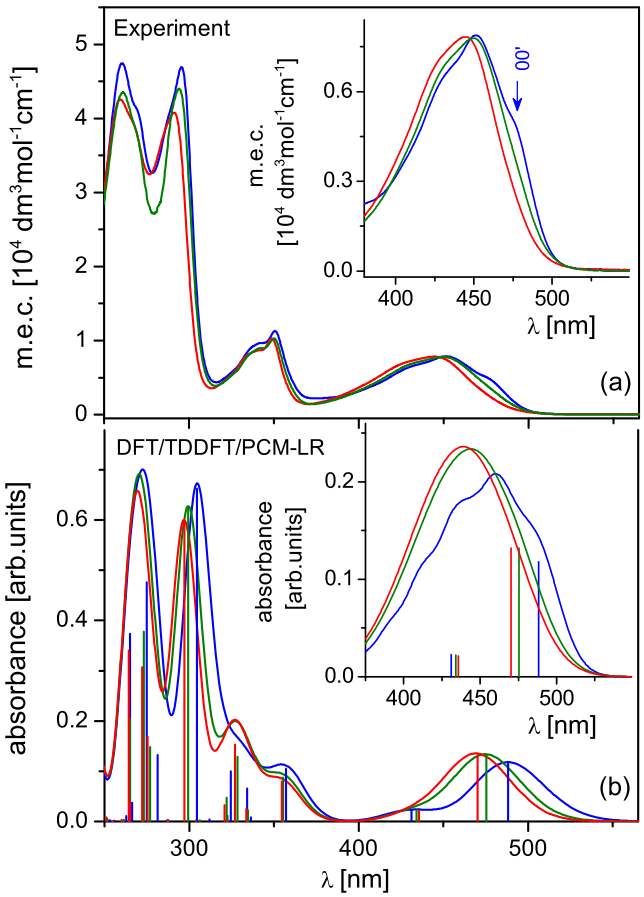

Fig. 4 The optical absorption spectra of DPIPQ. Panel **a** shows the measured spectra in CHX (*blue color* online), THF (*green color* online) and ACN (*red color* online) solutions; insert shows the first absorption band in details. Panel **b** shows the calculated spectra by DFT/TDDFT/PCM-LR in CHX (*blue color* online), THF (*green color* online) and ACN (*red color* online) solutions. The vertical lines are the oscillator strengths corresponding to the electronic transitions between the ground and excited singlet states ($\Gamma = 0$); the continuous lines simulate the optical absorption spectra by introducing the Gaussian lineshape broadening ($\Gamma = 0.25$ eV). The inserts in panel **b** shows the first absorption band calculated by means of Eq. 1 in CHX, THF and ACN solutions (see text for corresponding details)

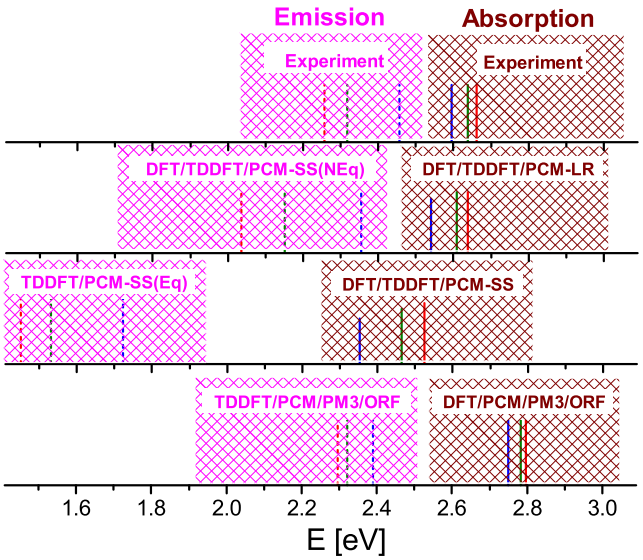

Fig. 5 Spectral positions of the first absorption bands ($0 \rightarrow 0'$ transition, *vertical solid lines*, right subsection) and fluorescent bands ($0' \rightarrow 0$ transition, *vertical dashed lines*, left subsection) being determined from the measured spectra and calculated within several approaches as specified by labels. Calculations relevant with the equilibrium or non-equilibrium states of the solute (as for the fluorescence emission only) are marked as Eq or NEq, respectively. *Blue*, *green* or *red colors* online corresponds to CHX, THF or ACN solutions, respectively

ground state solvent reaction field should be considered. DFT/TDDFT/PCM shows that it stabilizes better the ground state S_0, associated mainly with HOMO, rather than the excited state S_1 being related with LUMO. At the fluorescence emission one deals with the excited state solvent reaction field which acts just in an opposite way, i.e. it stabilizes better the excited state S_1 rather than the ground state S_0. The results of cyclic voltammetry measurements can be directly compared with DFT calculations for DPIPQ in the ACN solution as being the most appropriate in this case. As for the ground state geometry the DFT method gives the HOMO and LUMO levels equal −5.99 eV and −2.88 eV, respectively. For comparison, the cyclic voltammetry results to somewhat lower values, i.e. −6.194 eV and −3.434 eV, correspondingly. Such discrepancy may be attributed to the tolerance of the voltammetry measurements as well as the accuracy of the DFT/PCM calculations, basically due to a "static" feature of the DFT model. One must be noticed that the DFT method calculates the virtual and occupied molecular orbital (MOs) being suitable mainly for a crude evaluation of the electronic transition energies and their changes in a solvent environment. As for the HOMO-LUMO gap the TDDFT method provides usually more accurate result since it mixes pairs of the MOs and thereby

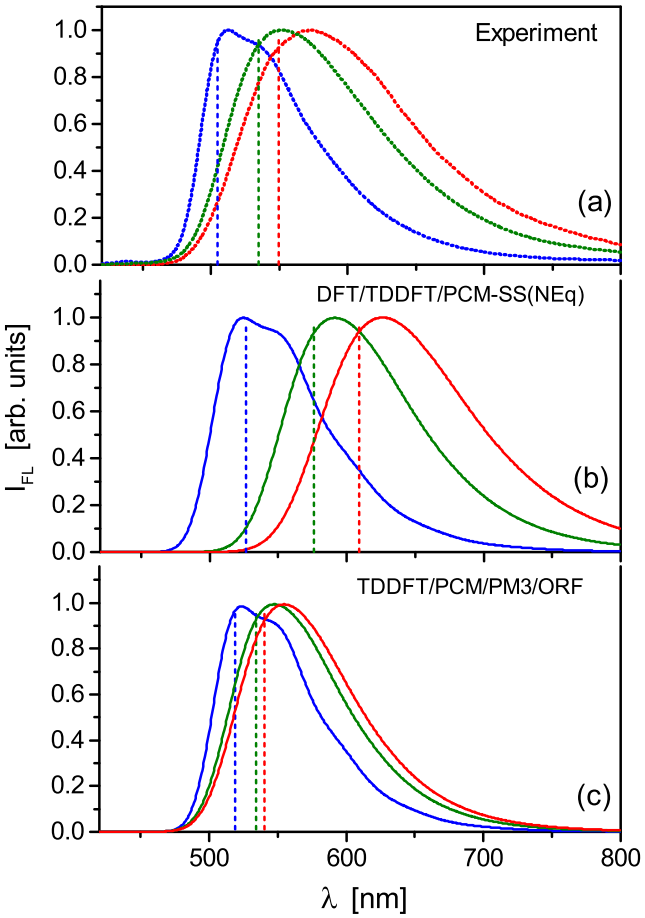

Fig. 6 The fluorescence spectra of DPIPQ in CHX (*blue color* online), THF (*green color* online) and ACN (*red color* online) solutions. Panel **a** refers to measured spectra. Panels **b** and **c** refer to calculated spectra by means of Eq. 3 using the magnitudes $E_{0'0}$, $\boldsymbol{\mu}_g(\boldsymbol{\mu}_g^*)$, $\boldsymbol{\mu}_e(\boldsymbol{\mu}_e^*)$ as evaluated within DFT/TDDFT/PCM-SS(NEq) or hybrid TDDFT/PCM/PM3/ORF approaches, respectively, and the common set of fit parameters: $S = 1.05$, $E_v = 1210$ cm^{-1}, $h_n = 0.10$ eV. *Vertical broken lines* indicate 0'→0 transition

accounts in a more correct way the electron correlation. On the other hand, within such calculations one deals with so called occupied and unoccupied natural transition orbitals (NTOs) which are not the same as virtual and occupied MO pairs obtained in the ground state calculations [29, 30] thus their direct comparison is not fully relevant.

The optical absorption and emission spectra were recorded in organic solutions with concentration of DPIPQ dye of about 10^{-5} M (it refers to absorbance of ca. 0.1 at excitation wavelength in the fluorescence). The measurements were performed by means of Shimadzu UV-VIS 2101 scanning spectrophotometer in the range of 230–600 nm using a standard 1 cm path length quartz cuvette for absorption spectrometry. To probe the solvatochromic effect on the absorption and fluorescence spectra, the measurements were carried out using CHX, THF and ACN as solvents. The solvents used in experiment were of HPLC grade. The steady state fluorescence spectra have been excited by a mercury lamp ($\lambda = 365$ nm) and recorded in a single photon counting mode. Further details regarding the technique used in spectroscopic measurements may be found in our recent paper [7]. Figure 4a shows the optical absorption spectra of DPIPQ measured in several solvents. They are unstructured in highly and medium polar solvents, although a certain structuring due to overlapped vibronic bands, spaced by about of 1,210 cm^{-1}, is evidently presented in the first optical absorption band in CHX solution. The first absorption maximum is centered at about 452 nm, however the electronic $0 \rightarrow 0'$ excitation, associated with the HOMO→LUMO transition, should be assigned to the kink-like shoulder observed at about 478 nm at the red wing of this band, see insert of Fig. 4a. Accordingly, the HOMO-LUMO gap obtained by the optical absorption method [$\Delta E_{\mathrm{HL}} = 2.59$ eV (CHX), 2.61 eV (THF) and 2.64 eV (ACN)], which is of about 0.12 eV smaller compared to the one measured by the cyclic voltammetry in ACN ($\Delta E_{\mathrm{HL}} = 2.76$ eV), basically well agrees with the TDDFT calculations. Figure 5 and Table 1 compare the spectral positions of the first absorption and fluorescence bands as being measured and calculated within several models. The DFT/TDDFT/PCM-LR or DFT/TDDFT/PCM-SS represent here the standard electronic structure calculations within the package G09-B01, being the combinations of the DFT method (ground state geometry optimization), TDDFT method (excitation spectra calculations) and the solvation models PCM-LR or PCM-SS, respectively. The PCM-SS approach refers to the lowest excited state of the solute in the ground state solvation reaction field. The DFT/TDDFT/PCM-SS(NEq) method calculates the fluorescence emission which takes place from the ground state molecular geometry, i.e. the same one as for the absorption process, but within the solvation reaction field relevant to the lowest excited state. Such nonstandard type of calculations indeed corresponds to the case of the solvation being in equilibrium with a non-equilibrium (unrelaxed) solute geometry in the excited state. It thereby highlights the mechanism of the solvent reorganization only excluding the effects caused by a solute reorganization in polar environment. In contrast to it, the TDDFT/PCM-SS(Eq) method represents again one of the standard approaches available within the package G09-B01 where the molecular structure optimization in the excited state likewise the fluorescent spectra calculation are performed using the TDDFT/PCM-SS method. Accordingly, it corre-

Table 1 Comparison of the spectroscopy characteristics of DPIPQ dye as obtained in the experiment and calculated within several quantum-chemical approaches

Method	Absorption			Fluorescence		
	CHX	THF	ACN	CHX	THF	ACN
Experiment						
λ_{max} [nm]	452 ± 1	449 ± 1	446 ± 1	511 ± 2	550 ± 2	572 ± 2
$E_{00'}\|E_{0'0}$ [eV]	2.596 ± 0.008	2.638 ± 0.008	2.661 ± 0.008	2.455 ± 0.015	2.317 ± 0.015	2.256 ± 0.015
DFT/TDDFT/PCM-LR						
$E_{00'}$ [eV]	2.539	2.608	2.637	–	–	–
$\Delta E_{00'}$ [eV]	−0.057	−0.03	−0.024	–	–	–
DFT/TDDFT/PCM-SS(NEq)						
$E_{0'0}$ [eV]	–	–	–	2.355	2.152	2.036
$\Delta E_{0'0}$ [eV]	–	–	–	–0.1	–0.165	−0.22
DFT/TDDFT/PCM-SS						
$E_{00'}$ [eV]	2.352	2.464	2.525	–	–	–
$\Delta E_{00'}$ [eV]	−0.244	−0.174	−0.136	–	–	–
TDDFT/PCM-SS(Eq)						
$E_{0'0}$ [eV]	–	–	–	1.722	1.532	1.451
$\Delta E_{0'0}$ [eV]	–	–	–	−0.733	−0.785	−0.805
DFT/PCM/PM3/ORF						
$E_{00'}$ [eV]	2.749	2.783	2.797	–	–	–
$\Delta E_{00'}$ [eV]	0.153	0.145	0.136	–	–	–
TDDFT/PCM/PM3/ORF						
$E_{0'0}$ [eV]	–	–	–	2.389	2.322	2.296
$\Delta E_{0'0}$ [eV]	–	–	–	−0.066	0.005	0.04

λ_{max} is the spectral peak position corresponding to the fluorescence or first absorption bands; $E_{00'}$ is 0→0' electronic transition energy (absorption process); $E_{00'}$ is 0'→0 electronic transition energy (emission process); $\Delta E_{00'}$ and $\Delta E_{0'0}$ are the differences (discrepancies) between the calculated and measured values

sponds to the case when the solvent reaction field and the solute geometry both reach their equilibrium in the excited state, i.e. fully relax prior a further vertical electronic transition into the final non-equilibrium ground state. The combinations DFT/PCM/PM3/ORF or TDDFT/PCM/PM3/ORF represent a hybrid approaches in which the molecular geometry is optimized by DFT/PCM (ground state, absorption process) or TDDFT/PCM (excited state, emission process) methods whereas the electronic spectra are calculated using the semiempirical method PM3 with further their correction within the solvation LM-ORF model.

All the methods properly predict the type of solvatochromism which accompanies the absorption-emission cycle. As for the absorption processes being considered, pure DFT/TDDFT methods exhibit also rather good quantitative agreement regarding the spectral position of the first absorption band defined by the 0→0' transition energy, $E_{00'}$. The discrepancy between the experiment and theory is here less than 0.06 eV for DFT/TDDFT/PCM-LR and 0.25 eV for DFT/TDDFT/PCM-SS, although the solvatochromic coefficients $dE_{00'}/dF$ (F is the solvent polarity) appear to be somewhat overestimated in both models, namely by the factors of 1.6 and 2.5, respectively. The hypsochromic trend of the first absorption band likewise the bathochromic trend for the fluorescence band appears to be also consistent with the vector diagram in Fig. 2a and b presenting the spatial orientation of the ground ($\boldsymbol{\mu}_g$ or $\boldsymbol{\mu}_g^*$) and lowest excited ($\boldsymbol{\mu}_e$ or $\boldsymbol{\mu}_e^*$) state dipole moments in the gas phase. An appropriate interpretation in this respect may be given within the ORF model [31] by means of the Lippert–Mataga [32, 33] equations. The latter ones define the solvatochromic corrections to the excitation ($E_{00'}$) or emission ($E_{0'0}$) energies as being proportional to the scalar products $\boldsymbol{\mu}_g(\boldsymbol{\mu}_g - \boldsymbol{\mu}_e)$ or $\boldsymbol{\mu}_e^*(\boldsymbol{\mu}_g^* - \boldsymbol{\mu}_e^*)$, respectively. Evidently, the blue shift of the first absorption band likewise the red shift of the fluorescence band in a polar solvent environment are caused by a specific orientation of dipole moments $\boldsymbol{\mu}_g(\boldsymbol{\mu}_g^*)$ and $\boldsymbol{\mu}_e(\boldsymbol{\mu}_e^*)$, i.e. appear to be consistent with the opposite signs of the above scalar products as it evidently follows from the vector diagrams given in Fig. 2.

Figure 4b presents the optical absorption spectra calculated by DFT/TDDFT/PCM-LR method. Here blue, green and red online colors correspond to CHX, THF and ACN solutions, respectively. The vertical lines are the oscillator strengths due to the electronic transitions between the singlet ground (S_0) and excited (S_i) states.

The continuous lines simulate the absorption spectra where corresponding bands are approximated by the Gaussian shape with the empirical parameter describing the bandshape broadening, Γ, equals to 0.25 eV. The DFT/TDDFT/PCM-LR method well reproduces the basic features of the measured spectra including the first absorption band in the region of 450 nm and two strong absorption bands in the UV-region at about 260 nm and 290 nm. However, the first absorption maximum, being calculated for several solvents, is slightly red shifted (25–40 nm) with respect to the measured one. The discrepancy should not be only attributed to the accuracy of DFT/TDDFT method but also to the fact that the vibronic coupling has been ignored in such calculations. Accounting the vibronic structure results to a more adequate description shown in inserts of Fig. 4b. The shape of the absorption bands has been modeled via the vibronic series similarly as [34–36]:

$$A(E) \propto \frac{M_a^2 E}{\sqrt{4\pi h_0 k_B T}} \sum_{j=0}^{\infty} \frac{e^{-S} S^j}{j!} \times \exp\left(-\frac{(E - E_{00'} - jE_v)^2}{4h_0 k_B T}\right) \quad (1)$$

where $A = \log(I_0/I)$ is the absorbance, M_a is the transition moment corresponding to the vertical transition from the ground state, S is the vibronic coupling constant, $E = h\nu$ is the excitation energy, E_v is the vibronic energy spacing, k_B is the Boltzmann constant, T is the temperature. The reorganization energy h_0 is related to the low-frequency motions such as reorientation of the solvent shell (h_s) as well as any other low-frequency and medium-frequency nuclear motions of the solute (h_n) and may be given by their sum as [34]:

$$h_0 = h_n + h_s = h_n + \frac{(\boldsymbol{\mu}_e - \boldsymbol{\mu}_g)^2}{a_0^3}\left(\frac{\varepsilon - 1}{2\varepsilon + 1} - \frac{n^2 - 1}{2n^2 + 1}\right) \quad (2)$$

Here the quantities S, E_v and h_n represent the model fit parameters given by the magnitudes 1.35, 1,210 cm^{-1} and 0.10 eV, respectively, what provides the best agreement with the shape of the first absorption band being measured in weakly polar CHX solution. All other quantities of interest, like e.g. the transition moment M_a, the transition energy $E_{00'}$, the ground state dipole moment $\boldsymbol{\mu}_g$ and the excited state dipole moment $\boldsymbol{\mu}_e$ have been directly determined in DFT/TDDFT or DFT/TDDFT/PCM calculations. The Onsager radius, a_0, is taken to be equal 0.57 nm as suggested by the molecular volume calculation within DFT method. The vibrational analysis shows, that the vibronic spacing, E_v, with the effective frequency of 1,210 cm^{-1} appears in the range of 1,100–1,500 cm^{-1} which corresponds to the modes consisting mostly of stretching vibrations, C-C, C-N or N-N bonds that form azafluoranthene or phenyl moieties.

As for the fluorescence emission being considered the conformational relaxation of the solute in the excited state should be taken into account. Usually it provides the red shift of the fluorescence emission already in the gas phase. The difference between the excitation and emission energies in the gas phase, $\Delta E_{a-f}^{gas} = E_{00'}^{gas} - E_{0'0}^{gas}$, gives a rough idea about the scale of purely conformational changes that happen with the solute during the absorption-emission cycle. The magnitudes $E_{00'}^{gas}$ and $E_{0'0}^{gas}$ can be also estimated from the spectra measured in solvents of different polarity F. Then, by extrapolating the spectral position of the optical absorption or emission bands into the region $F \to 0$ one obtains $\Delta E_{a-f}^{gas} \approx 0.07$ eV. The TDDFT analysis relevant to this case gives for the gas phase, $\Delta E_{a-f}^{gas} \approx 0.63$ eV, suggesting thus on considerably stronger conformational changes in the excited state. The reason for a such large discrepancy deserves a more detailed consideration. Following our recent studies [7] the fluorescence emission of DPIPQ in organic solvents of different polarity is characterized by the lifetime in the range of 6–12 ns. For the molecule in the excited state it is evidently long enough to reach new equilibrium prior the fluorescence emission. For this reason the emission from a non-equilibrium excited state is rather unlikely. More reliable explanation should refer to a quality of the geometrical optimization itself, namely in regards to the excited states which generally speaking may be not so good as for the ground states. Such opinion has been also supported by official representatives of the Gaussian Inc. developing the G09-B01 as used in the present study. Following [37] the problem consists in a restricted number of accurate experimental investigations to be able to assess how reliable TDDFT geometries are, in contrast to the DFT optimization being developed basing on the extensive experimental data available for ground state geometries. For instance, the DFT/TDDFT/PCM-SS(NEq) calculations, which refer to the optimized ground state molecular geometry completely ignoring the conformational relaxation in the excited state, give in comparison with the experiment just a bit underestimated energy for the fluorescence emission, namely by 0.1–0.22 eV only depending on the solvent polarity, see Fig. 5 and Table 1. This appears to be in contrast with the TDDFT/PCM-SS(Eq) approach, which results in a much worse agreement with the experiment. The discrepancy in the last case exceeds even 0.8 eV what leads to a conclusion

that the geometrical relaxation in the excited state, obtained within the TDDFT/PCM-SS(Eq) method appears to be relevant with the conformational changes being considerably much stronger than it is in reality. Surprisingly, but real equilibrium geometry in the excited state seems to be closer to the ground state geometry, as obtained within the DFT optimization, rather than to the one which follows from the excited state geometry optimization using the TDDFT method. Rather good agreement with the experiment provides also the hybrid approach being the combination of the TDDFT/PCM optimization with the semiempirical calculations using PM3 method and the solvation model LM-ORF (TDDFT/PCM/PM3/ORF approach). It predicts the wavelength for the fluorescence emission with the accuracy in the range of 0.04–0.07 eV. In contrast to DFT/TDDFT/PCM-SS(NEq) calculations the TDDFT/PCM/PM3/ORF approach gives the emission energy slightly underestimated in a weakly polar solvents, as e.g. CHX, and a bit overestimated in moderately or strongly polar solvents, like e.g. THF or ACN (Fig. 5, Table 1). On the other hand, the solvatochromic coefficients for the fluorescence emission, $dE_{0'0}/dF$, evaluated within the hybrid model, appears to be considerably smaller in comparison with the experimental magnitude, particularly by the factor of about 0.42. In comparison, the DFT/TDDFT/PCM-SS(NEq) gives overestimated its value by the factor of about 1.7. A real shape of the fluorescence band due to vibronic coupling may be reproduced similarly as for the optical absorption [34–36]:

$$I(E) \propto \frac{M_f^2 E^3}{\sqrt{4\pi h_0 k_B T}} \sum_{j=0}^{\infty} \frac{e^{-S} S^j}{j!} \times \exp\left(-\frac{(E - E_{0'0} + jE_v)^2}{4h_0 k_B T}\right) \quad (3)$$

where $I(E)$ is the fluorescence intensity, M_f is the fluorescence momentum. Figure 6 compares the measured fluorescence spectra (panel a) with the ones being calculated by means of Eq. 3 basing on TDDFT/PCM-SS(NEq) (panel b) and hybrid TDDFT/PCM/PM3/ORF (panel c) approaches. The vertical dashed lines corresponds to the vertical 0→0' transition. In the case of the measured fluorescence spectra the first vibronic band position has been determined in each case by the second derivative method. With the same model parameters, $S = 1.05$, $E_v = 1{,}210$ cm^{-1} and $h_n = 0.10$ eV, the shape of the fluorescence band may be well reproduced for both models in the solvents of different polarity. In the case of the semiempirical calculations the Onsager radius is taken to be equal 0.43 nm as suggested in [7]. Evidently, the TDDFT/PCM/PM3/ORF approach gives in this case the best agreement with the experiment. Also the DFT/TDDFT/PCM-SS(NEq) approach gives the reasonable spectra for fluorescent emission. Taking into account that the latter model refers to the equilibrium ground state geometry, one may conclude that the dominant influence on the fluorescence emission results mainly from the solvent reorganization in the excited state whereas the conformational relaxation of the solute is indeed weak.

Conclusion

In conclusion, we have presented here the DFT/TDDFT study on the electronic structure and spectral properties of the five-membered annulated diphenyl azafluoranthene derivative DPIPQ by applying solvation PCM and LM-ORF approaches at the B3LYP/6-31+G(d,p) level of theory. The results of calculations are compared with the experimental optical absorption and fluorescence spectra as well as with the cyclic voltammetry measurements.

In the case of the excitation process, the DFT/TDDFT/PCM methods exhibit rather good quantitative agreement regarding the spectral position of the first absorption band; the discrepancy between the experiment and theory is less than 0.06 eV (LR approach) and 0.25 eV (SS approach). For the fluorescence emission the standard TDDFT/PCM-SS calculations considerably underestimate the transition energy, on about of 0.8 eV. The discrepancy should be likely attributed to insufficient accuracy of the TDDFT optimization in the excited state. On the other hand, the TDDFT/PCM model, which refers to the equilibrium ground state geometry, demonstrates considerably much better agreement with the experimental data. The accuracy in such calculations appears in the range of 0.1–0.22 eV depending on the solvent polarity. This finding suggests that the dominant influence on the fluorescence emission in the solvent environment results mainly from the solvent reorganization in the excited state whereas the geometrical relaxation of the solute is indeed weak and may be ignored. Considering DPIPQ molecules in the polar solvents, all the TDDFT/PCM approaches give the bathochromic (red) shift for the fluorescence emission and the hypsochromic (blue) shift for the optical absorption in accordance with the experimental observation as well as the calculated ground and excited state dipole moments. However, the solvatochromic coefficients,

which characterize such shifts, appear to be somewhat overestimated compared to the measured ones.

Rather acceptable agreement with the experimental data provides also the hybrid approach being the combination of the TDDFT/PCM optimization and the semiempirical electronic structure calculations by PM3 method and solvation model LM-ORF (TDDFT/PCM/PM3/ORF approach). As for the fluorescence emission this method predicts the transition energies in different solvents with the accuracy better than 0.04–0.07 eV. Such result is less interesting in the quantum-chemical aspect basically due to different models to be used for the geometrical optimization and the electronic structure calculations. Nevertheless, it may be of considerable practical importance for the physical and/or chemical engineering dealing with a development of new fluorescent materials for a broad range of applications. Similar studies on other azafluoranthene derivatives would be quite desirable in order to verify real accuracy of the approaches used in the present work.

Acknowledgement The calculations have been carried out in Wrocław Centre for Networking and Supercomputing (http://www.wcss.wroc.pl), grant no. 160.

References

1. Sato Y, Mizoguchi T, Kudo Y, Ishida R (1981) Novel triazafluoranthene compound and processes for preparing the same. U.S. Patent 4,367,230. Chem Abstr 96:217867 (1981)
2. Asselin AA, Humber LG (1979) 10b-Azafluoranthene derivatives and precursors thereof. U.S. Patent 4,171,443. Chem Abstr 92:41918 (1979)
3. Toribio F, Galceran MT, Puignou LJ (2000) Separation of heteroaromatic amines in food products. Chromatogr B 747:171
4. Khan SI, Nimrod AC, Mehrpooya M, Nitiss JL, Walker LA, Clark AM (2002) Antifungal activity of eupolauridine and its action on DNA topoisomerases. Antimicrob Agents Chemother 46:1785
5. Wamberg MC, Hassan AA, Bond AD, Pedersen EB (2006) Intercalating nucleic acids (INAs) containing insertions of 6H-indolo[2,3-b]quinoxaline. Tetrahedron 62:11187
6. Danel KS, Gąsiorski P, Matusiewicz M, Całus S, Uchacz T, Kityk AV (2010) UV–vis spectroscopy and semiempirical quantum chemical studies on methyl derivatives of annulated analogues of azafluoranthene and azulene dyes. Spectrochim Acta A 77:16
7. Całus S, Danel KS, Uchacz T, Kityk AV (2010) Optical absorption and fluorescence spectra of novel annulated analogues of azafluoranthene and azulene dyes. Mater Chem Phys 121:477
8. Gąsiorski P, Danel KS, Matusiewicz M, Uchacz T, Kityk AV (2010) From pirazoloquinolines to annulated azulene dyes: UV–VIS spectroscopy and quantum chemical study. J Lumin 130:2460
9. Gąsiorski P, Danel KS, Matusiewicz M, Uchacz T, Vlokh R, Kityk AV (2011) Synthesis and spectroscopic study of several novel annulated azulene and azafluoranthene based derivatives. J Fluoresc 21:443
10. Danel KS, Wisła A, Uchacz T (2009) Unexpected intramolecular cyclization of 4-(2-halophenyl)pyrazolo[3,4-b]quinolines: formation of 5- and 7-membered rings from one starter. ARKIVOC X:71
11. Całus S, Gondek E, Danel A, Jarosz B, Pokladko M, Kityk AV (2007) Electroluminescence of 6-R-1,3-diphenyl-1*H*-pyrazolo[3,4-*b*]quinoline-based organic light-emitting diodes (R = F, Br, Cl, CH_3, C_2H_3 and $N(C_6H_5)_2$). Mater Lett 61:3292
12. Gondek E, Całus S, Danel A, Kityk AV (2008) Photoluminescence and electroluminescence of methoxy and carboethoxy derivatives of 1,3-diphenyl-1*H*-pyrazolo[3,4-*b*]quinoline. Spectrochim Acta A 69:22
13. Gondek E, Kityk IV, Danel A (2008) Some anthracene derivatives with *N*,*N*-dimethylamine moieties as materials for photovoltaic devices. Mater Chem Phys 112:301
14. Liu S, He P, Wang H, Shi J, Gong M (2009) A highly luminescent dinuclear Eu(III) complex based on 4,4′-bis (4″,4″,4″-trifluoro-1″,3″-dioxobutyl)-*o*-terphenyl for light-emitting diodes. Mater Chem Phys 116:654
15. Iwakuma T (2008) Azaaromatic compounds having azafluoranthene skeletons and organic luminescent devices made by using the same. U.S. Patent 20080206597
16. Frisch MJ, Trucks GW, Schlegel HB, Scuseria GE, Robb MA, Cheeseman JR, Scalmani G, Barone V, Mennucci B, Petersson GA, Nakatsuji H, Caricato M, Li X, Hratchian HP, Izmaylov AF, Bloino J, Zheng G, Sonnenberg JL, Hada M, Ehara M, Toyota K, Fukuda R, Hasegawa J, Ishida M, Nakajima T, Honda Y, Kitao O, Nakai H, Vreven T, Montgomery JA Jr, Peralta JE, Ogliaro F, Bearpark M, Heyd JJ, Brothers E, Kudin KN, Staroverov VN, Keith T, Kobayashi R, Normand J, Raghavachari K, Rendell A, Burant JC, Iyengar SS, Tomasi J, Cossi M, Rega N, Millam JM, Klene M, Knox JE, Cross JB, Bakken V, Adamo C, Jaramillo J, Gomperts R, Stratmann RE, Yazyev O, Austin AJ, Cammi R, Pomelli C, Ochterski JW, Martin RL, Morokuma K, Zakrzewski VG, Voth GA, Salvador P, Dannenberg JJ, Dapprich S, Daniels AD, Farkas O, Foresman JB, Ortiz JV, Cioslowski J, Fox DJ (2010) Gaussian 09, revision B.01. Gaussian, Inc., Wallingford, CT
17. Gondek E, Danel A, Kwiecień B, Nizioł J, Kityk AV (2010) Photoluminescence spectra of bisphenol A based pyrazoloquinoline dimers in different solvents: experiment and quantum chemical calculations. Mater Chem Phys 119:140
18. Koścień E, Gondek E, Pokladko M, Jarosz B, Vlokh RO, Kityk AV (2009) Photoluminescence of 1,3-dimethyl pyrazoloquinoline derivatives. Mater Chem Phys 114:860
19. Improta R, Barone V, Scalmani G, Frisch MJ (2006) A state-specific polarizable continuum model time dependent density functional theory method for excited state calculations in solution. J Chem Phys 125:054103
20. Improta R, Scalmani G, Frisch MJ, Barone V (2007) Toward effective and reliable fluorescence energies in solution by a new state specific polarizable continuum model time dependent density functional theory approach. J Chem Phys 127:074504
21. Tomasi J, Mennucci B, Cammi R (2005) Quantum mechanical continuum solvation models. Chem Rev 105:2999
22. Koścień E, Sanetra J, Gondek E, Danel A, Wisła A, Kityk AV (2003) Optical absorption measurements and quantum-chemical simulations on 1*H*-pyrazolo[3,4-*b*]quinoline derivatives. Opt Commun 227:115

23. Koścień E, Sanetra J, Gondek E, Jarosz B, Kityk IV, Ebothe J, Kityk AV (2005) Optical poling effect and optical absorption of cyan, ethylcarboxyl and tert-buthyl derivatives of 1*H*-pyrazolo[3,4-*b*]quinoline: experiment and quantum-chemical simulations. Spectrochim Acta A 61:1933
24. Calus S, Gondek E, Danel A, Jarosz B, Kityk AV (2006) Optical absorption of 1,3-diphenyl-1*H*-Pyrazolo[3,4-*b*]quinoline and its derivatives. Opt Commun 268:64
25. Całus S, Gondek E, Danel A, Jarosz B, Kityk AV (2007) Photoluminescence of 1,3-Diphenyl-1*H*-pyrazolo[3,4-*b*]quinoline and its derivatives: experiment and quantum chemical simulations. Opt Commun 271:16
26. Trasatti S (1986) The absolute electrode potential: an explanatory note. Pure Appl Chem 58:955
27. Pavlishchuk VV, Addison AW (2000) Conversion constants for redox potentials measured versus different reference electrodes in acetonitrile solutions at 25°C. Inorg Chim Acta 298:97
28. The HOMO and LUMO orbitals have been calculated by means of the program Gabedit representing a free Graphical User Interface for computational chemistry packages written by A.R. Allouche. It is available from http://gabedit.sourceforge.net/
29. Martin RL (2003) Natural transition orbitals. J Chem Phys 118:4775
30. Badaeva E, Albert VV, Kilina S, Koposov A, Sykorad M, Tretiak S (2010) Effect of deprotonation on absorption and emission spectra of Ru(II)-bpy complexes functionalized with carboxyl groups. Phys Chem Chem Phys 12:8902
31. Onsager L (1936) Electric moments of molecules in liquids. J Am Chem Soc 58:1486
32. Lippert E (1955) Dipolmoment und elektronenstruktur von angeregten molekulen. Z Naturforsch A10:541
33. Mataga N, Kaifu Y, Koizumi M (1955) The solvent effect on fluorescence spectrum, change of solute-solvent interaction during the lifetime of excited solute molecule. Bull Chem Soc Jpn 28:690
34. Kapturkiewicz A, Herbich J, Karpiuk J, Nowacki J (1997) Intramolecular radiative and radiationless charge recombination processes in donor-acceptor carbazole derivatives. J Phys Chem A 101:2332
35. Marcus RA (1989) Relation between charge transfer absorption and fluorescence spectra and the inverted region. J Phys Chem 93:3078
36. Gould IR, Young RH, Miller LJ, Albrecht AC, Farid S (1994) Electronic sructures of exciplexes and excited charge-transfer complexes. J Am Chem Soc 116:8188
37. Clemente FR (2011) Private communication (Technical Support Gaussian, Inc.), 31.03.2011